Journal of Micromechanics and Microengineering

PAPER • **OPEN ACCESS**

Precisely controlled batch-fabrication of highly sensitive co-resonant cantilever sensors from silicon-nitride

To cite this article: Ioannis Lampouras *et al* 2024 *J. Micromech. Microeng.* **34** 015005

OPEN ACCESS
IOP Publishing
Journal of Micromechanics and Microengineering
J. Micromech. Microeng. **34** (2024) 015005 (14pp)
https://doi.org/10.1088/1361-6439/ad0d80

Precisely controlled batch-fabrication of highly sensitive co-resonant cantilever sensors from silicon-nitride

Ioannis Lampouras[1,2], Mathias Holz[2], Steffen Strehle[2] and Julia Körner[1,*]

[1] Department of Electrical and Computer Engineering, Leibniz University Hannover, 30167 Hannover, Germany
[2] Institute of Micro- and Nanotechnologies, Microsystems Technology Group, Technische Universität Ilmenau, 98693 Ilmenau, Germany

E-mail: koerner@geml.uni-hannover.de

Received 29 August 2023, revised 27 October 2023
Accepted for publication 16 November 2023
Published 28 November 2023

Abstract

Dynamic-mode cantilever sensors are based on the principle of a one-side clamped beam being excited to oscillate at or close to its resonance frequency. An external interaction on the cantilever alters its oscillatory state, and this change can be detected and used for quantification of the external influence (e.g. a force or mass load). A very promising approach to significantly improve sensitivity without modifying the established laser-based oscillation transduction is the co-resonant coupling of a micro- and a nanocantilever. Thereby, each resonator is optimized for a specific purpose, i.e. the microcantilever for reliable oscillation detection and the nanocantilever for highest sensitivity through low rigidity and mass. To achieve the co-resonant state, the eigenfrequencies of micro- and nanocantilever need to be adjusted so that they differ by less than approximately 20%. This can either be realized by mass deposition or trimming of the nanocantilever, or by choice of dimensions. While the former is a manual and error-prone process, the latter would enable reproducible batch fabrication of coupled systems with predefined eigenfrequency matching states and therefore sensor properties. However, the approach is very challenging as it requires a precisely controlled fabrication process. Here, for the first time, such a process for batch fabrication of inherently geometrically eigenfrequency matched co-resonant cantilever structures is presented and characterized. It is based on conventional microfabrication techniques and the structures are made from 1 μm thick low-stress silicon nitride. They comprise the microcantilever and high aspect ratio nanocantilever (width 2 μm, thickness about 100 nm, lengths up to 80 μm) which are successfully realized with only minimal bending. An average yield of $>$80% of intact complete sensor structures per wafer is achieved. Desired geometric dimensions can be realized within $\pm$1% variation for length and width of the microcantilever and nanocantilever length, $\pm$10% and $\pm$20% for the nanocantilever width and thickness, respectively, resulting in an average variation of its eigenfrequency by 11%. Furthermore, the dynamic oscillation properties are verified by vibration experiments in a scanning electron microscope. The developed process allows for the first time the batch fabrication of co-resonantly coupled systems with predefined

* Author to whom any correspondence should be addressed.

properties and controlled matching states. This is an important step and crucial foundation for a broader applicability of the co-resonant approach for sensitivity enhancement of dynamic-mode cantilever sensors.

Supplementary material for this article is available online

Keywords: cantilever sensors, batch-fabrication, microfabrication, co-resonant sensitivity enhancement, geometric eigenfrequency matching, microcantilever and high aspect ratio nanocantilever, silicon nitride MEMS

1. Introduction

Cantilever-based sensors are widely used for analysis and characterization purposes covering many scientific areas from materials research to biology and gas sensing [1–6]. Thereby, either the changes of the cantilever's static bending or its dynamic oscillation behavior is harnessed to gather insights into samples or systems under investigation. In case of the dynamic mode, the cantilever is driven to oscillate at or close to its resonance frequency and changes of its amplitude, phase or frequency due to an external interaction are tracked. Through calibration, sometimes in conjunction with analytical models, the changes of oscillation properties can be used to quantify the external interaction, which typically is a force, force gradient or mass change [7, 8].

The sensitivity of such dynamic-mode cantilever sensors can be described by the obtainable frequency shift $\Delta\omega$ in response to an interaction (additional mass Δm or force/force gradient represented as a change of stiffness Δk):

$$\Delta\omega = \sqrt{\frac{k+\Delta k}{m_{\mathrm{eff}}+\Delta m}} - \sqrt{\frac{k}{m_{\mathrm{eff}}}} \tag{1}$$

and is dependent on the cantilever's properties stiffness k and effective mass m_{eff}. As equation (1) illustrates, detection of very small interactions requires a soft and lightweight cantilever. This is usually achieved by employing either very thin beams (thickness less than 1 μm) or reduced overall dimensions, i.e. nanocantilevers [9].

Oscillation detection is commonly based on laser optical methods such as deflectometry or interferometry, where a laser spot is focused at the free end of the cantilever to track its movement [10]. Very precise detection of the oscillatory state has furthermore been achieved by laser-Doppler vibrometry [11–13]. However, these detection concepts are space consuming due to the necessary equipment and require cantilever dimensions in the micrometer range (at least for the free end) to precisely focus the laser spot and gather a robust reflection signal. For smaller cantilevers, this becomes increasingly difficult and different means such as paddle structures or reflective coatings have been explored and used [10, 14, 15].

Other methods of oscillation detection include piezoelectric materials which allow self-sensing/self-actuating structures without optical components. However, they come at the cost of increased fabrication complexity, reduced signal-to-noise ratio and the necessary additional layers can increase the stiffness of the cantilever and therefore lower the achievable sensitivity [16–20].

Consequently, the aims of high sensitivity and reliable oscillation detection are contrary in their requirements for an optimal sensor, demanding a nanoscale cantilever on the one hand and a microscale cantilever on the other hand. Hence, a persisting challenge for sensor design arises as many applications, for example in scanning probe methods for material characterization, call for strongly increased sensitivity.

Several concepts have been developed to address this issue, including use of higher order bending modes or specifically tailored geometries [21–23]. Another approach is provided by a co-resonant concept, which makes use of coupling and eigenfrequency matching of a micro- and a nanocantilever [8]. Its immense potential has been demonstrated in various proof-of-principle investigations in magnetic force microscopy and cantilever magnetometry, e.g. for studying real-time magnetization reversal of individual Heusler nanoparticles [9, 24].

The main advantage of this concept is that the oscillation detection is realized on the microcantilever with established methods, hence the sensors can be used in any basic scanning force microscope. It does not require advanced oscillation transduction techniques such as interferometry. On the other hand, the sensitivity of the co-resonant cantilever sensor is mainly determined by the properties of the nanocantilever, i.e. its effective mass and stiffness. It can easily be made very small and soft in order to be susceptible to smallest external interactions (mass load, force or force gradient). Hence, the concept allows the combination of very high sensitivity with reliable and robust detectivity. A principle sketch of a co-resonant sensor structure is depicted in figure 1.

The distinction between a sensing (nanocantilever) and detection (microcantilever) part enables the integration of advanced functionality, such as self-sensing and self-actuation, into the microcantilever without a negative impact on the sensitivity of the sensor as this is mainly dependent on the nanocantilever properties. The co-resonant concept can therefore be an important contribution in extending the application range of dynamic-mode cantilever sensors towards use cases which demand high sensitivity but prevent optical oscillation detection, e.g. in opaque or liquid media.

The challenge of the concept lies in the complex interplay between sensor properties which is introduced by the co-resonance. In a single cantilever sensor, sensitivity, linearity and stability are mainly determined by the geometry,

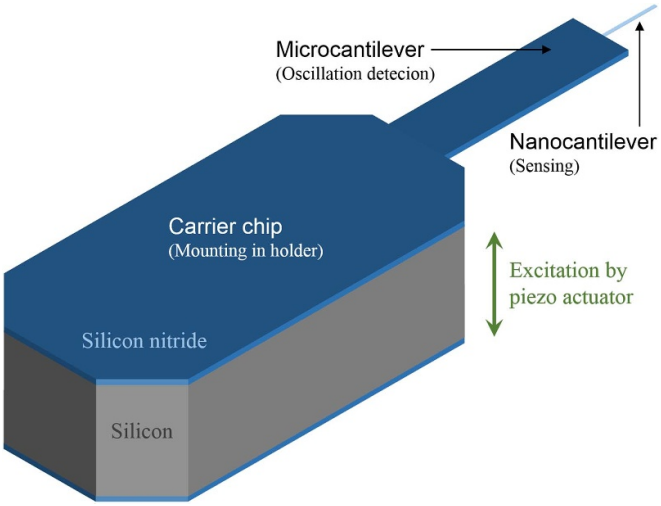

Figure 1. Principle sketch of a co-resonant sensor structure comprising the micro- and nanocantilever for oscillation detection and sensing, respectively, and a carrier chip for sensor mounting in a measurement head. The indicated materials are examples and refer to the ones used for the specific process development outlined in following section. Please note that the drawing is not to scale with regard to proportions for the sake of visibility. The carrier chip would normally be much larger than the cantilevers.

material, oscillation amplitude and the surrounding conditions (e.g. temperature, parasitic vibrations). In the co-resonant state, a multitude of effects, such as an amplitude amplification between micro- and nanocantilever, come into play besides the desired sensitivity increase. They can have a detrimental effect on the achievable sensor stability, resolution and linear range and therefore need to be carefully considered in the sensor design for a specific use case [9].

The only prerequisite for harnessing the co-resonant effect is the eigenfrequency matching between the micro- and the nanocantilever to the desired degree. This can either be achieved by mass deposition or trimming, or by specific adjustment of the cantilever dimensions. The former approach has been employed in all experiments to date, where individual sensors have been fabricated manually. However, the realization of predefined sensor properties by inherent geometric eigenfrequency matching holds great potential for application-specific design and batch fabrication capabilities. It also presents a significant challenge by requiring a highly precise fabrication process that overcomes several challenges associated with the co-resonance. In the following, the development and characterization of a suitable process and the successful batch-fabrication of co-resonantly coupled sensor structures with geometric frequency matching and predefined properties is described for the first time.

1.1. Basics of the co-resonant concept

The basis of the co-resonant principle is the eigenfrequency matching between a mechanically coupled micro- and nanocantilever. This approach leads to a system where an external influence at the highly sensitive nanocantilever affects the overall oscillation of the coupled system, which can be tracked at the microcantilever with established methods. Hence, the above mentioned contrary requirements are combined into a new sensor concept [7–9, 25].

To benefit from the co-resonance, it is necessary to adjust the eigenfrequencies to deviations of approximately less than 20% [9]. In this state, the sensor properties of the coupled system become a mix of the parameters of each individual cantilever with increasing dominance of the nanocantilever's properties for decreasing eigenfrequency deviation. Furthermore, for the coupled system, four relevant frequencies need to be distinguished: the individual eigenfrequencies of micro- and nanocantilever (f_m and f_n, respectively) and the two resonance frequencies of the coupled system (denoted as f_a and f_b for left and right resonance peak, respectively) [9]. The latter significantly differ from the individual beams' eigenfrequencies for close frequency matching.

The relevant eigenfrequency deviation Δf which needs to be adjusted to achieve co-resonance is defined as:

$$\Delta f = f_n - f_m \rightarrow \Delta f_{\mathrm{rel}} = \frac{f_n - f_m}{f_m} \cdot 100\% \tag{2}$$

in absolute and relative terms.

To realize a desired sensor performance with regard to sensitivity and detectivity the material and geometries of the coupled system need to be chosen and designed appropriately. In general, there are two approaches for eigenfrequency matching of micro- and nanocantilever to achieve the co-resonant state: either by adjusting the nanocantilever's effective mass (material deposition or trimming) or by geometric design of both cantilevers.

The latter is based on the following consideration: The eigenfrequency f_0 of a one-side clamped beam is given by [26]:

$$f_0 = \frac{1}{2\pi}\sqrt{\frac{k}{m_{\mathrm{eff}}}} \tag{3}$$

where k and m_{eff} denote dynamic spring constant and effective mass, respectively. These in turn can be expressed in terms of the geometrical and material properties of the cantilever, i.e. length l, width w, thickness t, second moment of area I, volume V, density ρ and Young's modulus E:

$$k \approx \frac{3EI}{l^3} \tag{4}$$

$$m_{\mathrm{eff}} = \frac{1}{4}\rho V. \tag{5}$$

Hence, the eigenfrequency becomes:

$$f_0 = \frac{1}{2\pi} \cdot \sqrt{\frac{12E}{\rho} \cdot \frac{I}{l^3 V}}. \tag{6}$$

As indicated by equation (6), volume, cross sectional area and length determine the eigenfrequency. Consequently, if the material properties of micro- and nanocantilever are set to be

the same, different combinations of dimensions can lead to the same eigenfrequencies of both beams. It is therefore possible to achieve a co-resonant state even if the nanocantilever for example has a very small thickness, which lends itself to high sensitivity.

So far, only the mass deposition and trimming approach has been used in co-resonantly coupled systems for experimental studies as the geometric eigenfrequency matching requires a very controlled fabrication of the cantilever dimensions.

The requirements of co-resonant coupling (i.e. very precise frequency matching to a desired degree and high sensitivity of the resulting sensor) pose several challenges for the fabrication process:

- High sensitivity requires a low-stiffness, hence very thin, nanocantilever while the microcantilever needs to be thicker and wider to ensure reliable oscillation detection. A sharp change of thickness (and geometric properties in general) at the transition point between both cantilevers is crucial to enable the co-resonance and a gradual or incremental change is not sufficient.
- Inherent geometric eigenfrequency matching in combination with high sensitivity (i.e. low spring constant) requires rather large aspect ratios of the nanocantilever due to its small thickness.
- To achieve specific sensor properties, a very controlled process is essential to realize well-controlled dimensions for a desired matching state. This is specifically relevant for the nanocantilever as even small alterations in thickness and/or length will have a significant influence on stiffness and frequency matching, respectively. Furthermore, the process needs to be stable and precise enough to enable batch fabrication of many sensors with consistent properties and low variance on one wafer as well as between individual wafers to ensure reproducibility.
- The desired thickness of the nanocantilever (in the order of few ten nanometers) makes it very fragile. Therefore, wet chemical processes should be avoided and replaced with dry processes where possible, e.g. for resist removal, and wafers handled very carefully throughout the fabrication.

Such a fabrication process would not only enable coupled systems with precisely matched eigenfrequencies but also provide the potential for batch fabrication of similar sensors—something that has not been possible so far.

1.2. State-of-the art of co-resonant sensor fabrication

So far, all reported experimental studies of the co-resonant approach have been conducted with individually built sensors consisting of commercially available silicon microcantilevers and multi-walled carbon nanotubes (MWCNTs) as nanocantilevers. Sensor fabrication was carried out manually in a dual scanning electron (SEM)/focused ion beam (FIB) system by transferring an MWCNT to the end of the microcantilever by means of a micromanipulator. After positioning the MWCNT in a way that its long axis was aligned with that of the microcantilever, the contact point between both was fixed by electron beam induced deposition of amorphous carbon through the gas injection system (GIS). This resulted in a mechanically coupled system but the eigenfrequencies of micro- and nanocantilever did not coincide due to their very different material and geometric properties.

To achieve eigenfrequency matching, a point mass was deposited at the free end of the nanocantilever by electron beam induced deposition of amorphous material (mainly platinum and carbon) with *in-situ* observation of the resonance frequencies [25]. Figure 2 depicts an exemplary coupled system in the as-fabricated and frequency matched state.

While this fabrication process allows precise matching of the eigenfrequencies through *in-situ* oscillation observation, it also has some major drawbacks:

- Influence of mass deposition on the nanocantilever's oscillation properties: While figure 2(c) depicts a rather extreme case for illustration purposes, usually a substantial amount of material has to be deposited at the nanocantilever's free end to lower its eigenfrequency towards that of the microcantilever. The additional mass needs to be distributed equally around the nanotube to avoid substantial distortion of the oscillation direction and mode shape.
- Mass deposition due to scanning with electron beam: Each time an image is taken, the electron beam scans over the sensor and deposits additional amorphous material from the gas residue and environmental contaminants left in the SEM chamber from GIS use. While not relevant for the microcantilever, it can notably influence the nanocantilever's eigenfrequency. Hence, every time the oscillation of the system is determined, it is slightly altered as well.
- Stability of the frequency matching state: While an adjusted eigenfrequency matching state is preserved inside the SEM chamber, it can change drastically when the sensor is removed from the vacuum and transferred to other equipment, e.g. an atomic force microscope, for actual sensor usage. The deposited material can contain open chemical bonds which can react with the environmental gases and therefore, the matching state is not stable and drifts over prolonged amounts of time. This results in unpredictable sensor properties undesired for sensor applications.
- Unpredictability of sensors properties: Due to the error proneness of the fabrication process, the aforementioned instability of the frequency matching state and the time-consuming manual assembly and adjustment, it is not possible to mass fabricate sensors with predefined properties, i.e. certain effective spring constant and hence, sensitivity.

These shortcomings of the current fabrication method constitute a major obstacle for wide-spread use of the co-resonant concept and consequently need to be resolved. The described process relies on eigenfrequency matching after mechanical coupling of the separately fabricated beams. However, based on the theoretical considerations outlined above it is possible to define coupled geometries with inherent eigenfrequency matching by choice of appropriate dimensions. Hence, neither manual coupling nor substantial additional mass deposition are required.

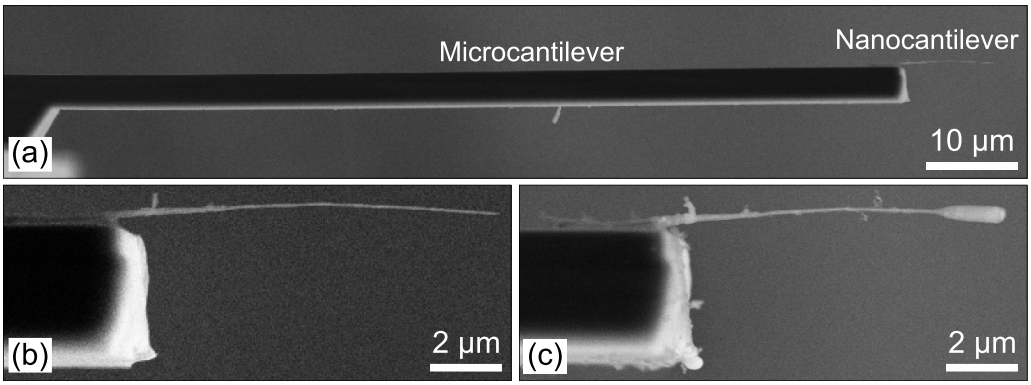

Figure 2. Scanning electron microscope image of an exemplary co-resonantly coupled system fabricated by manually combining a commercial silicon microcantilever and multi-walled carbon nanotube as nanocantilever. (a) Overview, (b) magnification of the nanocantilever at the free end of the microcantilever in the unmatched state, (c) eigenfrequency matching achieved by mass deposition at the free end of the nanocantilever.

1.3. Fabrication approaches for micro- and nanocantilevers

The focus of the work presented in the following is on the development of a batch process for reproducible fabrication of co-resonantly coupled cantilever sensors with predefined frequency matching by microstructuring techniques. While there are no reported processes that would address the specific challenges associated with the co-resonant concept, a lot of publications discuss techniques for fabrication of individual micro- and nanocantilevers and some also for coupled cantilevers. Since the developed process is based on this large fund of knowledge, a brief account of relevant ideas is given here.

Fabrication of single microcantilevers with thickness ranging from several μm down to the order of few ten nanometers can be found in many publications, e.g. [3, 27, 28], and is an established process for commercially available sensors. Usually a top-down approach is employed and cantilevers are either made from silicon (by use of silicon on insulator (SOI) wafers) or silicon nitride [29–31].

The fabrication of high-aspect ratio nanocantilevers, especially with precisely controlled dimensions, is much more challenging as these can become very fragile and tend to easily bend and stick to surfaces. Additionally, they are prone to be affected by even slight variations of process parameters [32, 33]. Therefore, one has to carefully adjust the order of process steps and choose appropriate techniques to avoid breakage, bending or complete loss of the structure due to, for example overetching or undercuts [34].

Previously reported fabrication approaches include thinning of the device layer of SOI wafers or silicon nitride membranes on silicon by reactive ion etching and subsequent release by oxygen plasma or hydrogen fluoride vapor. Thereby, cantilevers with thickness of (60–70) nm, widths of (1–10) nm and lengths of (5–120) μm have been fabricated [31].

Very precise control over dimensions has been achieved by masks created with ion implantation through FIB, resulting in silicon cantilevers with widths down to 25 nm, thicknesses below 100 nm and lengths of less than 10 μm [35, 36].

Much fewer publications describe the fabrication of coupled systems and in most cases, both cantilevers have similar dimensions [37–39]. Vidal-Álvarez *et al* reported the fabrication of a coupled system consisting of a silicon microcantilever and a silicon nanowire. In that case, the microcantilever was fabricated by a standard top–down approach while the nanowire was created afterwards from a gold catalyst particle by epitaxial growth [40]. While this fabrication process enables very good control of the nanowire's properties, it is not suitable for mass fabrication due to the requirement of positioning the catalyst particles at the end of the microcantilever (in [40] particles were distributed randomly).

In summary, batch fabrication processes for both, micro- and nanocantilevers have been reported, including means to precisely control dimensions, but to date no process is available to fabricate a combination of micro- and nanocantilever with the additional challenge of low variance to achieve optimal eigenfrequency matching of the two subsystems.

In the following, a process is outlined, which addresses the above described challenges and allows batch fabricating co-resonantly coupled systems on wafer-level with a predefined eigenfrequency matching state by choice of the dimensions. First, the target design is described, followed by a detailed account of the developed process. The work is concluded by an analysis of relevant parameters to evaluate the feasibility of the process for achieving the desired sensor properties.

2. Materials and methods for sensor fabrication and characterization

2.1. Choice of base material

As reported in many studies, silicon nitride is a well-suited material for thin cantilever and membrane fabrication due to its convincing mechanical, chemical and thermal stability [41, 42]. Silicon nitride thin films with a thickness in the range of (10–100) nm maintain their material properties, exhibit high flexibility and can be bent without breaking. Furthermore, the

material can be tailored with respect to its internal stress which enables highest quality factors ($>10^6$) for few ten nanometer thick resonators [43–45]. Low stress (i.e. residual stress compensated) silicon nitride is also beneficial for prevention of bending deformation in thin film cantilevers upon release from carrier structures [46, 47].

The material can be deposited on the surface of a silicon wafer and processed with conventional lithography and microfabrication methods such as wet chemical or reactive ion etching [48–50]. Furthermore, due to its resistance to potassium hydroxide (KOH), silicon nitride can be used as an etch stop layer [51].

For the presented sensor fabrication, low stress silicon nitride is chosen as base material for the coupled system due to these favorable properties, specifically the material stability after thin film release. Therefore, 4 inch single crystalline (100) p-type silicon wafers (thickness 380 ± 15 μm, TTV <10 μm, resistivity (1–10) Ω) coated on both sides with 1000 nm of low stress silicon nitride (deposited by low pressure chemical vapor deposition) are used (Microchemicals GmbH, Germany).

2.2. Sensor dimensions

To achieve geometric eigenfrequency matching, the dimensions of both cantilevers need to be chosen accordingly, while at the same time satisfying the requirements for high sensitivity (nanocantilever) and stable oscillation detection (microcantilever). For the development and characterization of the fabrication process, we are considering cantilevers with rectangular cross section, hence $V = l \cdot w \cdot t$ and $I = w \cdot t^3/12$ [52]. Combining this with equation (6), the cantilever's eigenfrequency is expressed by:

$$f_0 = \frac{1}{2\pi} \cdot \frac{t}{l^2} \cdot \sqrt{\frac{E}{\rho}}. \tag{7}$$

Furthermore, three different target frequency matching states have been chosen for evaluation of process yield and accuracy, i.e. $\Delta f = [0; -2.3; 5]\%$. Please note that in principle any matching state can be realized with the described process.

The dimensions for micro- and nanocantilever are based on commercially available sensors and previous work with carbon nanotube cantilevers which had diameters of (20–150) nm. Based on equation (7), the required lengths to reach the desired frequency matching state have been calculated and the resulting target dimensions are summarized in table 1. Thereby, the material properties of low-stress silicon nitride have been chosen as $E = 300$ GPa and $\rho = 3.1$ g cm^{-3} [53, 54].

2.3. Fabrication methods

Conventional micro- and nanostructuring methods are employed for the fabrication. The following techniques and machines are used for the main process steps:

Table 1. Target dimensions of micro- and nanocantilever with rectangular cross section for three different eigenfrequency deviations Δf_{rel} (only microcantilever length varied).

Parameter	Microcantilever	Nanocantilever
Cross section	rectangular	rectangular
Width w	40 μm	2 μm
Thickness t	1000 nm	100 nm
Length l, $\Delta f_{rel} = 0\%$	111 μm	35 μm
Length l, $\Delta f_{rel} = -2.3\%$	110 μm	35 μm
Length l, $\Delta f_{rel} = 5.0\%$	114 μm	35 μm

- UV laser lithography at 375 nm wavelength: Maskless Aligner MLA150, Heidelberg Instruments Mikrotechnik GmbH, Germany
- Reactive ion etching (RIE) with tetrafluoromethane (CF_4) and oxygen (O_2): Oxford RIE Plasmalab 100, Oxford Instruments Plasma Technology, UK
- Wet chemical etching of the silicon wafer by KOH
- Oxygen microwave plasma treatment: Tepla 200 Microwave Oxygen Plasma, PVA TePla AG Germany

All used photoresists (AZ series), developer and remover were purchased from MicroChemicals GmbH, Germany. Resist and remover were used as received and developer diluted with DI water as described below.

2.4. Characterization methods

The fabricated structures were characterized with optical and scanning electron microscopy with respect to their lengths and widths (optical microscope, Zeiss Primotech, Germany; FIB Nanoengineering Helios Nanolab 600i, Thermo Fisher Scientific Inc. USA; FIB Nanoanalytik Auriga 60, Zeiss, Germany). Profilometry (Tactile profilometer Dektak 150, Veeco Instruments Inc. USA) wass used to determine the nanocantilever thickness. The thickness of the initial silicon nitride was obtained with an ellipsometer (UV–Vis–NIR-Ellipsometer SenResearch 4.0, Sentech, Germany). Thereby, measurements were carried out at five spots on the wafer (middle, north, south, east and west) with an angle of 60° and 70° between source and detector. The corresponding fitting curve of these 10 data points was calculated based on a model comprising four layers (from top to bottom): roughness of silicon nitride surface, low stress silicon nitride, native silicon dioxide and silicon.

3. Fabrication process

The developed fabrication process for co-resonantly coupled structures from silicon nitride comprises the following main steps:

(i) Photolithography on wafer front and back side: On the front, the photomask defines the microcantilever geometry and the area where the silicon nitride will be thinned to form the nanocantilever and surrounding area.

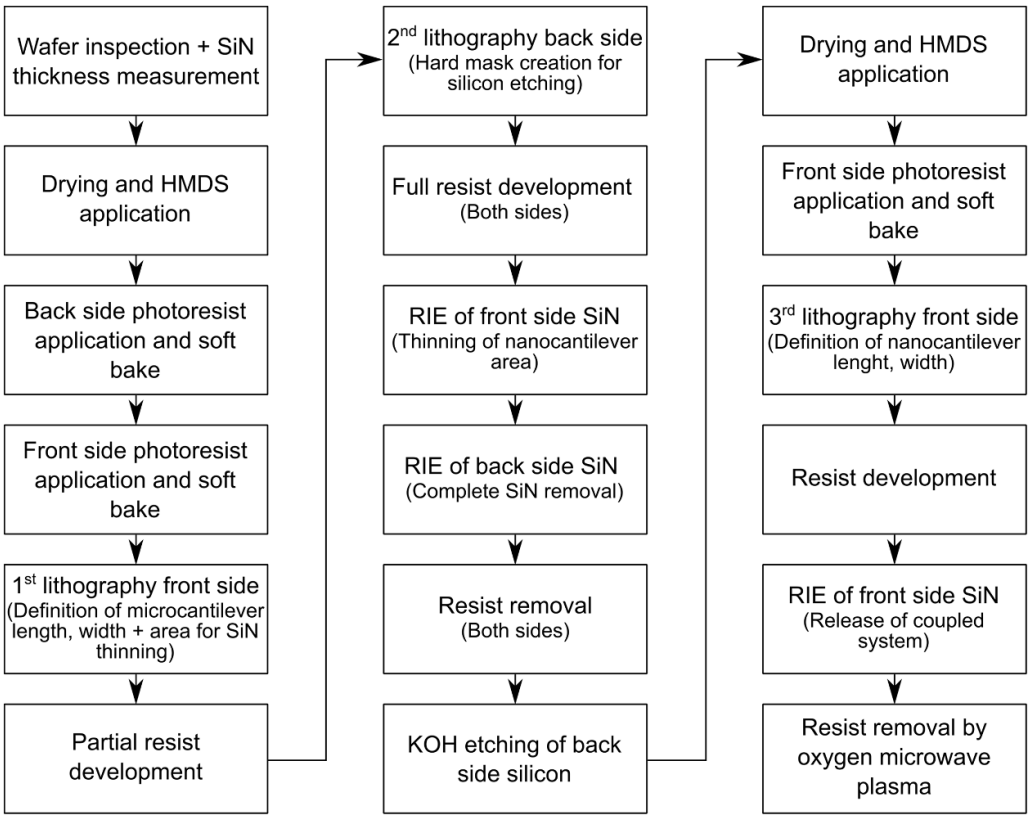

Figure 3. Flow chart of the most important process steps for batch fabrication of geometrically eigenfrequency matched co-resonantly coupled systems. A detailed account of all process steps and parameters is given in the supporting information.

On the back side, the window for release of the coupled cantilever structure is defined.

(ii) Thinning of the front side silicon nitride around the microcantilever and in the area of the nanocantilever to the desired target thickness by dry etching.

(iii) Complete removal of the back side silicon nitride in the sensor area by dry etching

(iv) Removal of back side silicon to create a suspended and partially thinned silicon nitride membrane comprising the coupled structure.

(v) Photolithography (direct laser writing) to define nanocantilever geometry and subsequent simultaneous nanocantilever formation and release of complete coupled structure by dry etching of front side silicon nitride

Figures 3 and 4 depict a flow chart of the main steps and graphical representations of the intermediate structures. A detailed account of all fabrication steps and process parameters can be found in the supporting information. In the following, the main aspects of the process are discussed.

3.1. Step (i): definition of geometry

First of all, the thickness of the silicon nitride layer on the wafer is measured by ellipsometry as this will be used to determine the necessary etching duration for subsequent process steps.

After visual inspection with an optical microscope and subsequent drying by air evaporation in a furnace (105 °C for 30 min), hexamethyldisilazane (HMDS) is applied to both sides of the wafer by a CVD process (at 95 °C) as an adhesion promoter for the photoresist. Positive resist AZ 1518 is spin-coated on the wafer back side followed by a soft bake at 100 °C for 30 s in nitrogen atmosphere. The same resist is then applied to the front side of the wafer using the same spin-coating protocol, followed by further soft bake of the wafer at 100 °C for 45 s in nitrogen atmosphere.

After 2 min rehydration of the approx. 1.8 μm thick photoresist in clean room air, the wafer front side is exposed by direct laser writing lithography to define the microcantilever outline and nanocantilever area, followed by a partial development in AZ developer (1:1 dilution with DI water) for 15 s. This is stopped by immersion of the wafer in DI water and serves to make the alignment marks visible for the back side structuring. Next, the wafer back side is exposed by direct laser writing lithography to define the complete sensor area. After that, the resist is fully developed on both sides in AZ developer (1:1 dilution with DI water) for 35 s.

3.2. Step (ii): nanocantilever area thinning

The nanocantilever as well as the surrounding area on the wafer front side as defined by the photoresist in step (i) is thinned to the desired target value by reactive ion etching with

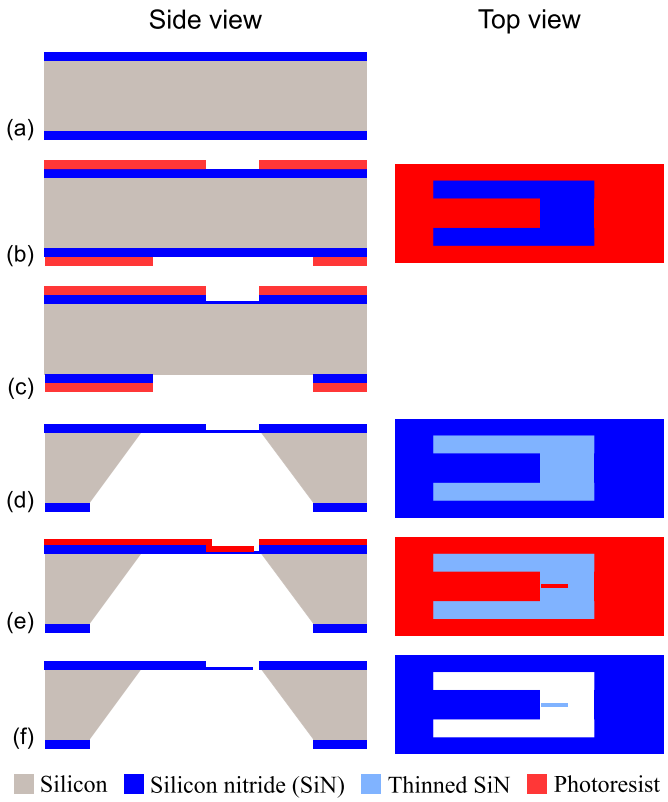

Figure 4. Fabrication process flow for co-resonantly coupled sensor in silicon nitride: (a) Initial silicon wafer with both sides coated with 1 μm low-stress silicon nitride. (b) Application of photoresist on both sides of the wafer and photolithographic definition of microcantilever outline and nanocantilever area (front side) and complete sensor area (back side). (c) Thinning of nanocantilever area to desired thickness (front side) and complete etching of silicon nitride to expose silicon (back side) with reactive ion etching. (d) Stripping of photoresist and KOH etching of back side silicon to suspend the silicon nitride membrane. (e) Front side lithography for definition nanocantilever length and width. (f) Structuring of nanocantilever and release of the complete sensor structure by reactive ion etching and subsequent photoresist removal by oxygen microwave plasma ashing.

CF_4 (35 sccm) and O_2 (3 sccm) at 200 W, pressure of 75 mTorr (10 Pa) and controlled temperature of 20 °C. This is a critical step with respect to process control because it requires a high accuracy and constant etching rate. The etching time is adjusted according to the measured initial silicon nitride thickness (approx. 915 nm) and is 5 min 55 s for the presented geometry with a target 100 nm thickness. The target value must be reached as precisely as possible to achieve the desired eigenfrequency matching state.

This step defines the geometry (length, width) of the microcantilever and the thickness of the nanocantilever. The accuracy of achieving the target values has been checked by microscopic analysis and profilometry during process development.

3.3. Step (iii): back side silicon nitride opening

Reactive ion etching with the same gases and process parameters as before is then performed on the wafer back side for 8 min to open the silicon nitride layer and expose the silicon underneath. Afterwards, the photoresist is removed with AZ 100 remover from both sides and the wafer rinsed with DI water and spin dried.

Please note that these first three steps of silicon nitride structuring can also be carried out subsequently on front and back side. First for front side: application of resist, exposure, development, RIE etching to thin the nanocantilever area and resist removal. Then for the back side: resist application, exposure (after aligment to marks on front side), development, RIE etching to open silicon nitride layer to expose silicon and resist removal.

As we had to be considerate about the number of process steps, the presented approach with parallel processing of both sides and partial photoresist development was chosen. The results described below clearly indicate that this is feasible and leads to the desired sensor structures.

3.4. Step (iv): back side silicon removal

The back side silicon is removed by a wet chemistry etching step. Therefore, the wafer is placed in 40% wt. KOH solution at 80 °C for 8 h and 30 min. In order to avoid mechanical stress specifically in the thin silicon nitride on the front side, the wafer is tempered in 60 °C warm DI water for 5 min before the etching and immersed in initially 70 °C DI water for 30 min after the process, followed by DI water rinsing and spin drying.

3.5. Step (v): nanocantilever formation and coupled structure release

In this step, the nanocantilever's lenght and width are defined and the complete coupled structure released by through etching of the suspended silicon nitride membranes at the structure's edges.

Therefore, again HMDS is applied to the wafer front side by a CVD process (at 95 °C) as adhesion promoter for the photoresist. Next, positive resist AZ 1505 is spin-coated on the wafer front side, followed by a soft bake for 60 s at 100 °C in nitrogen atmosphere.

To prevent damage of the fragile silicon nitride membranes due to the vacuum holder of the lithography instrument, the wafer is attached to a silicon support wafer by paraffin wax before exposure. After photoresist exposure, the support wafer is removed (see details in supporting information) and the resist developed in AZ 351B developer (1:4 dilution with DI water) for 35 s.

The release of the sensor structure is achieved by reactive ion etching for 1 min and 5 s with CF_4 (35 sccm) and O_2 (3 sccm) at 200 W, pressure of 75 mTorr (10 Pa) and temperature of 20 °C. Please note that the photoresist is stabilizing the nanocantilever during this step and should therefore not be too thick to avoid mechanical stress on the nanocantilever.

The last and most critical step is the photoresist removal as any wet chemistry would very likely damage the nanocantilever. Therefore, oxygen microwave plasma ashing (15 min at 300 W) is used to remove the photoresist.

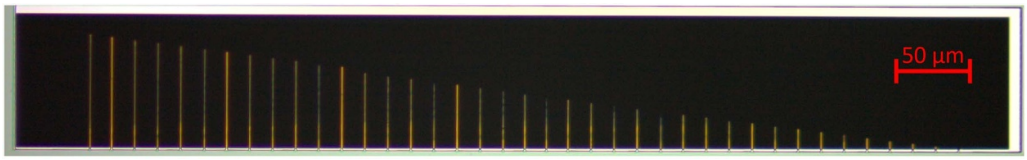

Figure 5. Top view of an array of silicon nitride nanocantilevers with varying lengths from 2 μm to 80 μm (increment of 2 μm), constant width of 1 μm and thickness of 100 nm. The image was taken by an optical microscope with 50× magnification.

Table 2. Yield of finalized fabrication process for a total of seven wafers each containing 63 co-resonant sensors.

Wafer	Yield (Absolute)	Yield (Percentage)
W1	62/63	98.4%
W2	60/63	95.2%
W3	44/63	69.8%
W4	40/63	63.0%
W5	46/63	73.0%
W6	54/63	86.0%
W7	63/63	100.0%
Total	369/441	83.6%

4. Results and discussion

4.1. Stability test for nanocantilever fabrication

Precise adjustment of the nanocantilever length is crucial for obtaining a desired frequency matching state. Furthermore, one major challenge of the process is to keep the nanocantilever intact during all steps. In order to study the feasibility of the proposed fabrication process and determine the potential stable range of 100 nm thick silicon nitride structures, 63 arrays of nanocantilevers only (without the microcantilever) were fabricated on one wafer with the above described process. The nanocantilever width was kept constant at 1 μm while the length was varied from 2 μm to 80 μm in increments of 2 μm (resulting in 39 cantilevers per array). The fabricated arrays were visually inspected afterwards for integrity of the cantilevers. Figure 5 depicts an optical microscope image of one array.

It is found that 33.3% of the arrays (21 out of 63) are fully intact, i.e. all nanocantilever lengths could successfully be preserved. Furthermore, 61.9% have at least 20 intact nanocantilevers (50% yield), including the longest one with 80 μm.

From this experiment it is concluded that the fabrication process is capable of preserving the structural integrity of high aspect-ratio nanocantilevers (100 nm thickness, 2 μm width) of lengths up to 80 μm.

4.2. Complete system fabrication

4.2.1. Yield of intact sensors. In order to evaluate the process yield with respect to integrity of the complete cantilever system, seven wafers each containing 63 co-resonantly coupled structures of identical target dimensions for 0% eigenfrequency deviation were fully processed and optically inspected afterwards. From 441 fabricated systems, 369 were fully intact, i.e. both cantilevers successfully fabricated and preserved, which is an overall yield of 83.6%. The details for each wafer are listed in table 2.

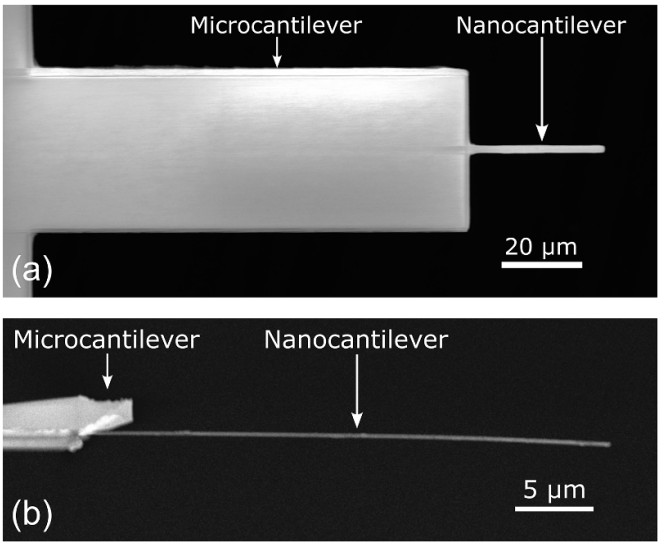

Figure 6. Scanning electron microscope image of (a) top and (b) side view of an exemplary co-resonantly coupled system made from silicon nitride and based on the dimensions listed in table 1. Please note that in (b) only the free end of the microcantilever is visible.

Figure 6 depicts a SEM image of an exemplary fabricated co-resonantly coupled system with the target dimensions for 0% eigenfrequency deviation listed in table 1. It is clearly visible that the nanocantilever's stability is maintained throughout the process and only very slight bending is visible, despite an aspect ratio of 324 (length 35 μm, thickness 108 nm). All intact sensors looked similar and no severe bending of the nanocantilever was observed.

4.2.2. Oscillation properties of fabricated sensor. To verify that the fabricated sensors exhibit the desired oscillation behavior which is characterized by two resonance peaks as described in the introduction, they have been placed on a home-built vibration stage and studied in a SEM. Thereby, the sensor is excited by a shear piezo actuator driven with an external sinusoidal voltage with fixed amplitude and varying frequency. For each frequency, an SEM image is captured and the amplitudes of the cantilevers measured afterwards. Details of the vibration stage and the procedure can be found in the supporting information and in [25].

Table 3. Properties of the exemplary sensor depicted in figure 7. The dimensions have been obtained as described above, the eigenfrequencies calculated with equation (7) and the coupled resonance frequencies f_a and f_b determined based on [9].

Parameter	Microcantilever	Nanocantilever
Width	39.5 μm	2 μm
Length	103.1 μm	34 μm
Thickness	0.9884 μm	0.1034 μm
Eigenfrequency	145.58 kHz	139.63 kHz
	Calculation	
f_a	138.47 kHz	
f_b	146.80 kHz	
Spacing	8.33 kHz	
	Measurement	
f_a	105.8 kHz	
f_b	114.8 kHz	
Spacing	9.00 kHz	

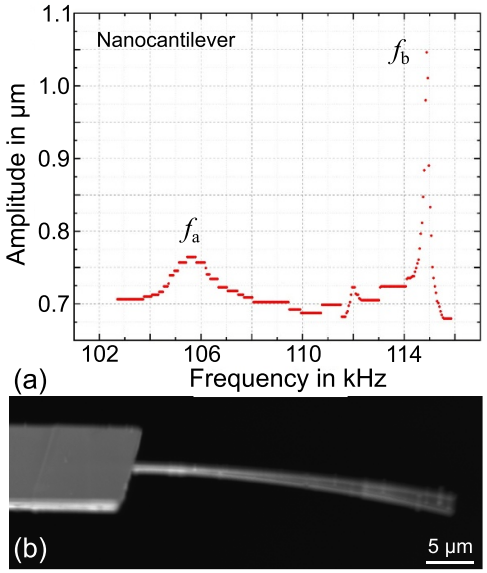

Figure 7. (a) Amplitude response curve of an exemplary fabricated co-resonantly coupled system (properties listed in table 3) obtained by measuring the amplitude of the nanocantilever in individual scanning electron microscope (SEM) images at different excitation frequencies (the detailed procedure is outlined in [25]. The two expected resonance peaks of the coupled system are clearly visible ($f_a \approx 105.8$ kHz, $f_b \approx 114.8$ kHz). (b) SEM image (stage tilted by 10°) of that sensor excited at the second resonance frequency $f_{exc} = f_b$. Only the free end of the microcantilever is shown and it exhibits a much smaller amplitude than the nanocantilever due to the expected amplitude amplification [8]. Please note that the sensor has been covered with 2 nm of platinum to reduce charging effects in the SEM.

Figure 7 depicts the amplitude response curve of an exemplary sensor obtained by measuring the amplitude of the nanocantilever and a corresponding SEM image for sensor excitation at the second coupled resonance peak f_b. The complete set of sensor properties comprising geometric dimensions, calculated and measured resonance frequencies, is listed in table 3.

Based on the measured sensor dimensions the eigenfrequencies of micro- and nanocantilever can be calculated with equation (7) and the coupled resonance frequencies with the formulas from [9]. Compared to the theoretical resonance frequencies, the measured ones are notably lower but the spacing between f_a and f_b is almost the same. The origin of the reduced frequencies is likely due to process related geometric deviations which could not be determined from the measurements of the cantilever dimensions, such as flank angle or underetching. This needs to be studied further and potentially be integrated into future sensor design considerations.

Overall, the sensor clearly shows the expected behavior known from previous studies (e.g. [24, 25]) and it can therefore be concluded that the fabrication process is feasible for realizing the desired co-resonant oscillation properties.

4.2.3. Evaluation of process accuracy with respect to target dimensions. The eigenfrequency matching state of the coupled system is crucial for its dynamic oscillation behavior and consequently sensor properties. Especially the nanocantilever length and thickness need to be precisely fabricated in order to reach the predefined matching to the microcantilever's eigenfrequency. Furthermore, for batch fabrication it is important that the variation throughout the wafer is as low as possible to maximize the output of coupled systems exhibiting co-resonant behavior.

In order to evaluate the developed process with respect to precision and variation, a batch of six wafers was processed, each one containing 63 coupled systems. Thereby, two wafers each were designed for 0%, −2.3% and 5% eigenfrequency deviation according to the dimensions listed in table 1. A total of 376 structures were then measured with respect to their resulting dimensions by optical microscopy (length, width), ellipsometry (microcantilever thickness from initial wafer thickness) and profilometry (nanocantilever thickness after thinning by RIE). Based on these dimensions, the eigenfrequencies of micro- and nanocantilever were calculated with equation (7) for $E = 300$ GPa and $\rho = 3.1$ g cm^{-3} [53, 54].

The results are summarized as box plots in figure 8. Wafers represented with the same base color have identical target dimensions for 0% (grey), −2.3% (orange) and 5% (green) eigenfrequency deviation and the black horizontal lines indicate the target values. The frequency matching is realized by adjusting the microcantilever length as visible in figure 8(a).

The microcantilever thickness (figure 8(c)) is not depicted as box plots as it has been obtained from ellipsometry measurements of the initial wafer's silicon nitride layer. As described in section 2.4, this is done by fitting a material model to the data of 5 measurement spots with 2 angles of incidence each, hence 10 data points. The output is the depicted fitting value and corresponding standard error for thickness.

For the microcantilever, the target length and width can be realized with good accuracy and similar variation among wafers. However, the thickness was found to be smaller than the expected 1000 nm of the purchased wafers which

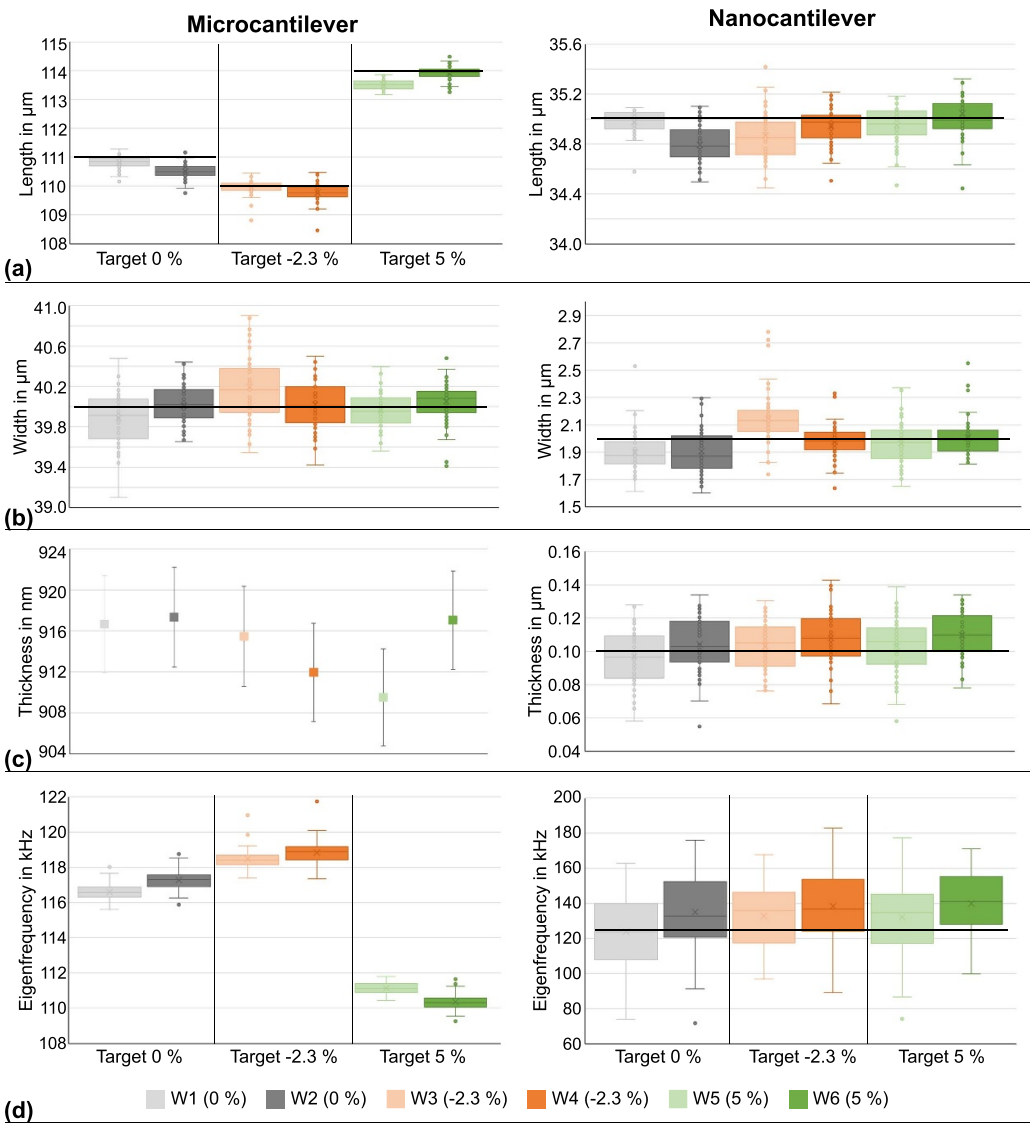

Figure 8. Box plots of (a) length, (b) width, (c) thickness and (d) eigenfrequency distribution of micro- and nanocantilever for each wafer. Wafers with the same base color have identical target dimensions for 0% (grey), −2.3% (orange) and 5% (green) eigenfrequency deviation. The black horizontal lines in all figures (except for microcantilever in (c) and (d)) indicate the target values as listed in table 1. Please note that the microcantilever thickness in subfigure (c) is not depicted as box plot but instead as mean value and standard error. This is due to the measurement of this thickness by ellipsometry which fits the model of the wafer surface stack to 5 measurement spots (see section 2.4).

substantially lowers the resulting eigenfrequencies. The mask for sensor fabrication was designed for 1000 nm thickness of the microcantilever which would lead to eigenfrequencies of (123; 126; 117) kHz for eigenfrequency deviations of (0; −2.3; 5)%. As visible in figure 8(d), the resulting eigenfrequencies are significantly lower due to this thickness error.

For the nanocantilever, the geometry is the same for all structures, as the frequency matching is realized through adjustment of the microcantilever length. The variations on each wafer and among wafers are similar and the target dimension can be realized with good accuracy. The thickness variation has the largest influence on the resulting eigenfrequencies (target value 124 kHz) as also indicated by equation (7).

Based on the calculated eigenfrequencies, the matching state of each fabricated sensor can be determined as the eigenfrequency deviation according to equation (2) and the yield of matching state ranges is summarized in figure 9. Regardless of the target value, all wafers show a similar distribution of eigenfrequency deviations. This can be attributed to the reduced thickness of the microcantilever which adds a systematic offset and shifts the desired matching states of (0; −2.3; 5)% to (10; 8; 16)%. Therefore, the matching states and distributions are very similar for figures 9(a) and (b) but for 9(c) a clear shift of the distribution to the right, i.e. higher deviations, is visible. This is due to the real target matching state being 16%.

From these evaluations it can be concluded that the approach of geometric eigenfrequency matching can be realized with the developed process and enables the fabrication of sensors with predefined co-resonant properties. The above

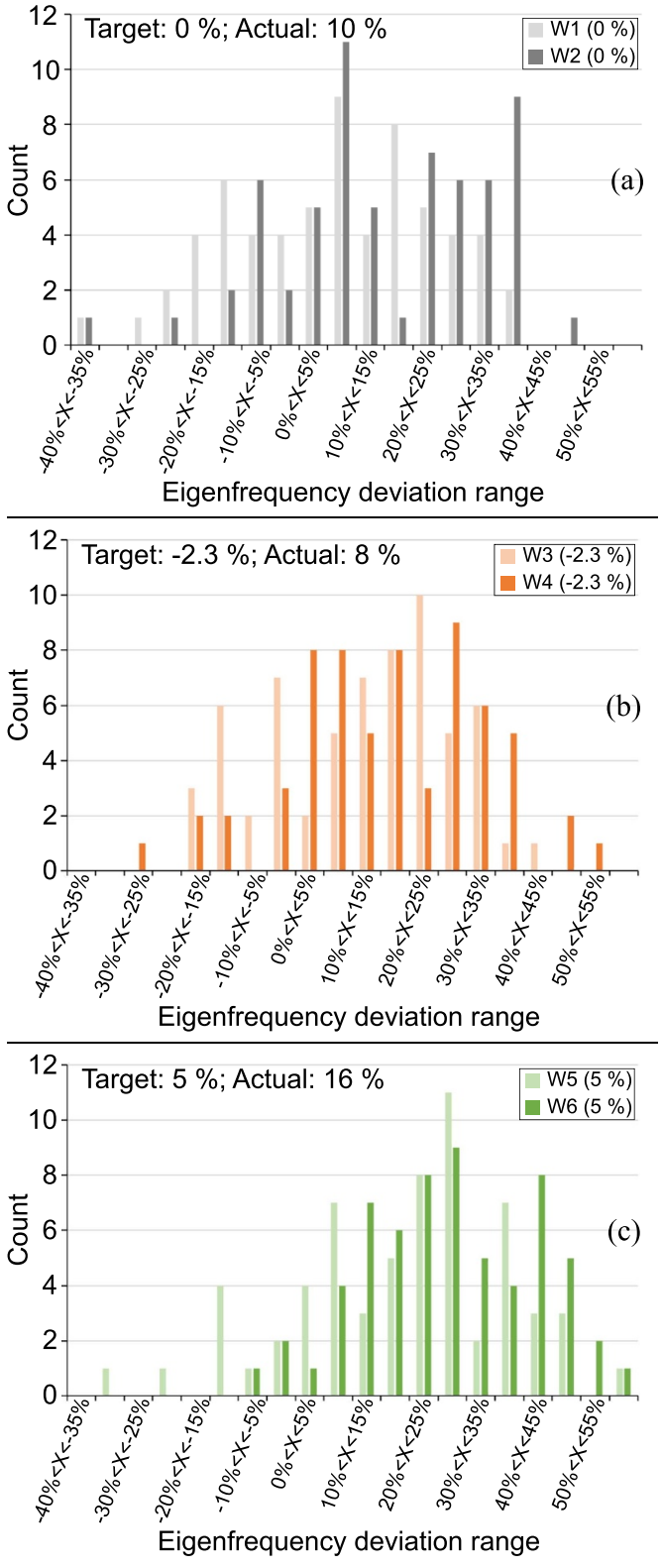

Figure 9. Number of sensors per wafer with the indicated eigenfrequency matching ranges for six processed wafers, each containing 63 structures. The count is based on calculation of the micro- and nanocantilever eigenfrequencies from their geometric dimensions and the corresponding eigenfrequency deviations by equations (7) and (2). At least two-thirds of sensors per wafer fulfill the criteria for co-resonance, i.e. eigenfrequency deviations between micro- and nanocantilever of less than 20%.

results furthermore highlight the importance of thorough pre-characterization of the initial silicon nitride (especially with regard to thickness) and the consideration in the geometry and mask design.

5. Conclusion

The fabrication of cantilever sensors exhibiting sensitivity enhancement through co-resonance requires precise eigenfrequency matching of a coupled micro- and a nanocantilever. The sensitivity of such a sensor is mainly determined by the nanocantilever's properties, increasingly so for decreasing eigenfrequency deviation. The desired eigenfrequency matching can be achieved by two different strategies: (a) mass deposition on or trimming of the nanocantilever, or (b) appropriate choice of geometric dimensions for both cantilevers to reach inherent coincidence of the eigenfrequencies. The former is a manual, time-consuming and error prone process with unpredictable and barely reproducible sensor properties. Despite these shortcomings, it has been successfully used for all experimental proof-of-principle studies exploring the potential of the co-resonant concept so far. However, it is not suitable for batch fabrication and wide-spread sensor use.

The second strategy of geometric design enables very stable and precise sensor properties but is challenging with respect to fabrication due to (i) sharp change of dimensions (specifically thickness, but also width) at the transition point between both cantilevers (a gradual changes would not be sufficient) and (ii) necessary large aspect ratio of the nanocantilever due to the requirements of high sensitivity (i.e. thickness of few ten nm) and matching to the microcantilever's eigenfrequency (i.e. lengths of several 10 μm).

In the presented investigation, a batch process for fabrication of geometrically eigenfrequency matched co-resonantly coupled systems based on silicon nitride is developed and characterized. It enables the creation of 100 nm thick and 1 μm wide nanocantilevers with lengths ranging from (2–80) μm, i.e. aspect ratios between 20–800, with minimal bending along the length.

The process yield of intact sensor structures amounts to $>$80% per wafer. The accuracy in achieving target dimensions is $\pm$1% for length and width of the microcantilever and nanocantilever length, $\pm$10% and $\pm$20% for the nanocantilever width and thickness, respectively. This leads to a variation of the nanocantilever's eigenfrequency by $\pm$11%. Based on a comprehensive analysis of several hundred sensor structures it is concluded that the developed process is suitable for batch-fabrication of co-resonantly coupled systems with desired properties which has furthermore been verified by first vibration experiments of fabricated sensors.

The presented results clearly indicate the potential for mass production capabilities of the developed process and furthermore underline the necessity of thorough wafer pre-characterization and precise control of fabrication parameters. By being able to determine the eigenfrequency matching state through geometry, co-resonantly coupled sensors with

predefined properties can now be fabricated with good reproducibility which is an important milestone for future applications of the co-resonant principle for sensitivity enhancement.

As a next step, comprehensive analysis of the dynamic oscillation properties of fabricated sensor structures with different eigenfrequency matching states will be performed to study the achievable sensor properties and compare them to calculated and simulated data. One specifically interesting aspect is the transition between linear and non-linear bending regimes and the potential consequences for sensor stability and linearity, which are crucial for applications.

Data availability statement

The data cannot be made publicly available upon publication because no suitable repository exists for hosting data in this field of study. The data that support the findings of this study are available upon reasonable request from the authors.

Acknowledgments

Funding of the presented research by the German Research Foundation (Deutsche Forschungsgemeinschaft DFG, Grant Number KO5508/3-1) is gratefully acknowledged. This work was carried out at the Center of Micro- and Nanotechnologies of TU Ilmenau and we would like to thank Arne Albrecht, Christian Koppka, Manuela Breiter, Henry Romanus, Andrea Knauer for their experimental support and technical assistance. Furthermore, we thank Christopher Reiche for critical review of the manuscript.

ORCID iDs

Ioannis Lampouras https://orcid.org/0000-0003-2083-2667
Mathias Holz https://orcid.org/0000-0003-4526-5726
Steffen Strehle https://orcid.org/0000-0002-1261-2894
Julia Körner https://orcid.org/0000-0001-6516-9462

References

[1] Larsen T, Schmid S, Grönberg L, Niskanen A O, Hassel J, Dohn S and Boisen A 2011 Ultrasensitive string-based temperature sensors *Appl. Phys. Lett.* **98** 121901
[2] Leahy S and Lai Y 2017 A cantilever biosensor exploiting electrokinetic capture to detect *Escherichia coli* in real time *Sens. Actuators* B **238** 292–7
[3] Stowe T D, Yasumura K, Kenny T W, Botkin D, Wago K and Rugar D 1997 Attonewton force detection using ultrathin silicon cantilevers *Appl. Phys. Lett.* **71** 288–90
[4] Tabata O, Kawahata K, Sugiyama S and Igarashi I 1989 Mechanical property measurements of thin films using load-deflection of composite rectangular membranes *Sens. Actuators* **20** 135–41
[5] Johnson B N and Mutharasan R 2012 Biosensing using dynamic-mode cantilever sensors: a review *Biosens. Bioelectron.* **32** 1–18
[6] Baller M K *et al* 2000 A cantilever array-based artificial nose *Ultramicroscopy* **82** 1–9
[7] Körner J, Reiche C F, Gemming T, Büchner B, Gerlach G and Mühl T 2016 Signal enhancement in cantilever magnetometry based on a co-resonantly coupled sensor *Beilstein J. Nanotechnol.* **7** 1033–43
[8] Reiche C F, Körner J, Büchner B and Mühl T 2015 Introduction of a co-resonant detection concept for mechanical oscillation-based sensors *Nanotechnology* **26** 335501
[9] Körner J 2018 Effective sensor properties and sensitivity considerations of a dynamic co-resonantly coupled cantilever sensor *Beilstein J. Nanotechnol.* **9** 2546–60
[10] Nichol J M, Hemesath E R, Lauhon L J and Budakian R 2008 Displacement detection of silicon nanowires by polarization-enhanced fiber-optic interferometry *Appl. Phys. Lett.* **93** 193110
[11] Maier F J, Schneider M, Ullmann P, Hafner J and Schmid U 2021 α-phase PVDF MEMS cantilever excited by electrostriction and evaluated up to 160 °C in air by laser Doppler vibrometry *J. Appl. Phys.* **129** 214507
[12] Ohler B 2007 Cantilever spring constant calibration using laser Doppler vibrometry *Rev. Sci. Instrum.* **78** 063701
[13] O'Donoughue P *et al* 2023 Comparison of three full-field optical measurement techniques applied to vibration analysis *Sci. Rep.* **13** 3261
[14] DeMartini B E, Rhoads J F, Shaw S W and Turner K L 2007 A single input–single output mass sensor based on a coupled array of microresonators *Sens. Actuators* A **137** 147–56
[15] Gil-Santos E, Ramos D, Martínez J, Fernández-Regúlez M, García R, San Paulo A, Calleja M and Tamayo J 2010 Nanomechanical mass sensing and stiffness spectrometry based on two-dimensional vibrations of resonant nanowires *Nat. Nanotechnol.* **5** 641–5
[16] Adams J D, Parrott G, Bauer C, Sant T, Manning L, Jones M, Rogers B, McCorkle D and Ferrell T L 2003 Nanowatt chemical vapor detection with a self-sensing, piezoelectric microcantilever array *Appl. Phys. Lett.* **83** 3428–30
[17] Hwang I-H and Lee J-H 2006 Self-actuating biosensor using a piezoelectric cantilever and its optimization *J. Phys.: Conf. Ser.* **34** 362–7
[18] Lee S S and White R M 1996 Self-excited piezoelectric cantilever oscillators *Sens. Actuators* A **52** 41–45
[19] Lee Y, Lim G and Moon W 2007 A piezoelectric micro-cantilever bio-sensor using the mass-micro-balancing technique with self-excitation *Microsyst. Technol.* **13** 563–7
[20] Rogers B *et al* 2003 Mercury vapor detection with a self-sensing, resonating piezoelectric cantilever *Rev. Sci. Instrum.* **74** 4899–901
[21] Leahy S and Lai Y 2017 A gap method for increasing the sensitivity of cantilever biosensors *J. Appl. Phys.* **122** 064502
[22] Liao H-S, Huang K-Y and Chang C-S 2011 Cantilever-based mass sensor using high order resonances for liquid environment *2011 IEEE/ASME Int. Conf. on Advanced Intelligent Mechatronics (AIM) (Budapest, Hungary)* pp 652–5
[23] An S, Kim B, Kwon S, Moon G, Lee M and Jhe W 2018 Bifurcation-enhanced ultrahigh sensitivity of a buckled cantilever *Proc. Natl Acad. Sci.* **115** 2884–9
[24] Körner J, Reiche C F, Ghunaim R, Fuge R, Hampel S, Büchner B and Mühl T 2017 Magnetic properties of individual Co_2FeGa Heusler nanoparticles studied at room temperature by a highly sensitive co-resonant cantilever sensor *Sci. Rep.* **7** 8881
[25] Körner J 2018 A highly sensitive co-resonant cantilever sensor for materials research: application to nanomaterial characterization *J. Mater. Res.* **33** 2504–14
[26] Meirovitch L 1975 *Elements of Vibration Analysis* (McGraw Hill)

[27] Yasumura K Y, Stowe T D, Chow E M, Pfafman T, Kenny T W, Stipe B C and Rugar D 2000 Quality factors in micron- and submicron-thick cantilevers *J. Microelectromech. Syst.* **9** 117–25
[28] Li X, Ono T, Lin R and Esashi M 2003 Resonance enhancement of micromachined resonators with strong mechanical-coupling between two degrees of freedom *Microelectron. Eng.* **65** 1–12
[29] Yu Q, Qin G, Darne C, Cai C, Wosik W and Pei S-S 2006 Fabrication of short and thin silicon cantilevers for AFM with SOI wafers *Sens. Actuators* A **126** 369–74
[30] Harley J A and Kenny T W 1999 High-sensitivity piezoresistive cantilevers under 1000 Å thick *Appl. Phys. Lett.* **75** 289–91
[31] Yang J, Ono T and Esashi M 2000 Mechanical behavior of ultrathin microcantilever *Sens. Actuators* A **82** 102–7
[32] Corletto A and Shapter J G 2020 Nanoscale patterning of carbon nanotubes: techniques, applications and future *Adv. Sci.* **8** 2001778
[33] Oikonomou A, Clark N, Heeg S, Kretinin A, Varey S, Yu G and Vijayaraghavan A 2015 Scalable bottom-up assembly of suspended carbon nanotube and graphene devices by dielectrophoresis *Phys. Status Solidi* **9** 539–43
[34] Nilsen M, Port F, Roos M, Gottschalk K-E and Strehle S 2019 Facile modification of freestanding silicon nitride microcantilever beams by dry film photoresist lithography *J. Micromech. Microeng.* **29** 025014
[35] Brugger J, Beljakovic G, Despont M, de Rooij N F and Vettiger P 1997 Silicon micro/nanomechanical device fabrication based on focused ion beam surface modification and KOH etching *Microelectron. Eng.* **35** 401–4
[36] Sievilä P, Chekurov N and Tittonen I 2010 The fabrication of silicon nanostructures by focused-ion-beam implantation and TMAH wet etching *Nanotechnology* **21** 145301
[37] Gil-Santos E, Ramos D, Jana A, Calleja M, Raman A and Tamayo J 2009 Mass sensing based on deterministic and stochastic responses of elastically coupled nanocantilevers *Nano Lett.* **9** 4122–7
[38] Wang D F, Itoh T, Ikehara T and Maeda R 2012 Doubling flexural frequency response using synchronised oscillation in a micromechanically coupled oscillator system *Micro Nano Lett.* **7** 717
[39] Ono T, Tanno K and Kawai Y 2014 Synchronized micromechanical resonators with a nonlinear coupling element *J. Micromech. Microeng.* **24** 025012
[40] Vidal-Álvarez G *et al* 2015 Top-down silicon microcantilever with coupled bottom-up silicon nanowire for enhanced mass resolution *Nanotechnology* **26** 145502
[41] Hampshire S 2007 Silicon nitride ceramics–review of structure, processing and properties *J. Achiev. Mater. Manuf. Eng.* **24** 43–50 (available at: https://api.semanticscholar.org/CorpusID:137859447)
[42] Zwickl B M, Shanks W E, Jayich A M, Yang C, Bleszynski Jayich A C, Thompson J D and Harris J G E 2008 High quality mechanical and optical properties of commercial silicon nitride membranes *Appl. Phys. Lett.* **92** 103125
[43] Chakram S, Patil Y S, Chang L and Vengalattore M 2014 Dissipation in ultrahigh quality factor SiN membrane resonators *Phys. Rev. Lett.* **112** 127201
[44] Verbridge S S, Parpia J M, Reichenbach R B, Bellan L M and Craighead H G 2006 High quality factor resonance at room temperature with nanostrings under high tensile stress *J. Appl. Phys.* **99** 124304
[45] Verbridge S S, Craighead H G and Parpia J M 2008 A megahertz nanomechanical resonator with room temperature quality factor over a million *Appl. Phys. Lett.* **92** 013112
[46] Kandpal M, Behera S N, Singh J, Palaparthy V and Singh S 2020 Residual stress compensated silicon nitride microcantilever array with integrated poly-Si piezoresistor for gas sensing applications *Microsyst. Tech.* **26** 1370–85
[47] Novak A V, Novak V R, Dedkova A A and Gusev E E 2018 Dependence of mechanical stresses in silicon nitride films on the mode of plasma-enhanced chemical vapor deposition *Semiconductors* **52** 1953–7
[48] Loewenstein L M and Tipton C M 1991 Chemical etching of thermally oxidized silicon nitride: comparison of wet and dry etching methods *J. Electrochem. Soc.* **138** 1389–94
[49] Carlsen A T, Briggs K, Hall A R and Tabard-Cossa V 2017 Solid-state nanopore localization by controlled breakdown of selectively thinned membranes *Nanotechnology* **28** 085304
[50] Li J, Stein D, McMullan C, Branton D, Aziz M J and Golovchenko J A 2001 Ion-beam sculpting at nanometre length scales *Nature* **412** 166–9
[51] Williams K R, Gupta K and Wasilik M 2003 Etch rates for micromachining processing—part II *J. Microelectromech. Syst.* **12** 761–78
[52] den Hartog J P 1952 I Kinematik der Schwingungen *Mechanische Schwingungen* (Springer) pp 1–29
[53] Kaushik A, Kahn H and Heuer A H 2005 Wafer-level mechanical characterization of silicon nitride MEMS *J. Microelectromech. Syst.* **14** 359–67
[54] Khan A, Philip J and Hess P 2004 Young's modulus of silicon nitride used in scanning force microscope cantilevers *J. Appl. Phys.* **95** 1667–72